European Journal of Pharmaceutical Sciences 174 (2022) 106185

Contents lists available at ScienceDirect

European Journal of Pharmaceutical Sciences

journal homepage: www.elsevier.com/locate/ejps

Exploring bulk volume, particle size and particle motion definitions to increase the predictive ability of *in vitro* dissolution simulations

Marina Navas-Bachiller [a], Tim Persoons [b], Deirdre M. D'Arcy [a,*]

[a] School of Pharmacy and Pharmaceutical Sciences, Trinity College Dublin, Ireland
[b] Department of Mechanical, Manufacturing & Biomedical Engineering, Trinity College Dublin, Ireland

ARTICLE INFO

Keywords:
API dissolution simulations
Bulk volume
Sink conditions
Dissolution
In silico simulation

ABSTRACT

The definition of the local dissolution environment is central to accurate particle dissolution simulation, and is determined by the apparatus and conditions used. In the flow-through apparatus dissolution occurs in the cell, often in a low velocity environment, with the reservoir considered the relevant volume for dissolution kinetics. Dissolution simulations were conducted using a reduced-order model based on the Ranz-Marshall correlation for mass transfer from spherical particles. Using ibuprofen as a model drug, the effect of defining a local volume to simulate dynamic bulk concentration conditions in the flow-through and paddle apparatus was assessed by comparing use of a near particle volume (NPV), extending a distance of one radius from the particle surface, with a flow-through apparatus cell volume or paddle apparatus vessel volume as the relevant instantaneous volume for dissolution. The instantaneous inlet concentration to NPV or cell volume is the reservoir/vessel concentration at that simulation time point, reflecting the continuous input to the cell of more dilute solution from the reservoir (closed system). Additionally, inputting particle size distribution (PSD) instead of a median particle size (MPS) and enabling or disabling particle motion were investigated, in two media (resulting in low and high solubility) and with two fluid velocity conditions in each apparatus.

The NPV predicted effects of fluid velocity differences on dissolution in the high solubility medium in the flow-through apparatus, but had no effect on predictive ability in the paddle apparatus. In both apparatuses, simulations were reasonable for the high solubility environment but underpredicted dissolution in the low solubility environment. The PSD option and disabling particle motion increased the predictive ability of the simulations in low solubility media in the flow-through apparatus. The results highlight the necessity to incorporate the local dynamic dissolution conditions in the flow-through apparatus for accurate dissolution simulation, and the challenges of defining an effective particle size for dissolution simulation and of reflecting hydrodynamic complexity in simulating dissolution in the paddle apparatus.

1. Introduction

Dissolution simulation models build from theoretical mathematical equations that predict the dissolution rate of an active pharmaceutical ingredient (API) based on inputs describing the particle, fluid and other dissolution-related parameters (Sugano, 2009). They can help select *in vitro* conditions, serve as inputs for pharmacokinetic modelling and assess how manufacturing changes affect the dissolution profile (Pathak et al., 2017). Many models have been described in literature (Wang and Flanagan, 1999; Hintz and Johnson, 1989; Johnson, 2012; Sugano, 2008). Wang et al., 2012 considered the influence of bulk definition on dissolution simulation. They defined confinement as the increase in bulk concentration as a result of particles being present in a limited bounded volume or container. Confinement can be negligible when bulk concentration is very small compared to solubility which can be the case if the volume available for the particle to dissolve is very large or the drug is highly soluble. In dissolution testing, a drug mass is dissolved into a reservoir volume that is considered the relevant bulk volume, that is, the

Abbreviations: NPV, near-particle volume; PSD, particle size distribution; MPS, median particle size; API, active pharmaceutical ingredient; BCS, Biopharmaceutical Classification System; DCS, Developability Classification System; USP, United States Pharmacopeia; FDA, Food and Drug Administration; HPMC, Hydroxypropyl methylcellulose; PE, Predictive Error; RMSE, Root Mean Square Error.

* Corresponding author. The School of Pharmacy and Pharmaceutical Sciences. Panoz Institute. Trinity College Dublin, The University of Dublin. Dublin 2. Ireland. D02PN40

E-mail addresses: navasbam@tcd.ie (M. Navas-Bachiller), persoont@tcd.ie (T. Persoons), ddarcy@tcd.ie (D.M. D'Arcy).

https://doi.org/10.1016/j.ejps.2022.106185
Received 11 October 2021; Received in revised form 22 March 2022; Accepted 4 April 2022
Available online 6 April 2022

volume available for the particle to dissolve into at any instant in time. Bulk concentration can have a large influence on dissolution rate and it is not instantaneously uniform throughout the dissolution medium, as drug molecules diffuse in a time-dependent manner, according to Fick's law of diffusion (Bergman et al., 2011)(Mills, 1999). Bulk concentration is affected by mass dissolved, although simulation models can assume zero bulk concentration in sink conditions or mass dissolved in just one volume (Siepmann and Siepmann, 2013).

In the flow-through apparatus, the reservoir would normally be considered the relevant volume for bulk concentration, but dissolution occurs in the cell (D'Arcy et al., 2010; Todaro et al., 2017). However, even the flow-through cell volume could be considered an over-prediction of the effective available volume and may overestimate the dissolution rate. Providing a simulated near-particle volume (NPV) (Fig. 1), could render the simulated profile more accurate when the drug initially dissolves in a limited volume due to the low local fluid velocity regions and then diffuses through the cell and reservoir volumes .

An NPV was implemented and explored in the mechanistic simulation code, SIMDISSO^{TM}, which has been previously described (D'Arcy and Persoons, 2019, 2011). SIMDISSO^{TM} operates in Matlab (The MathWorks Inc.), but is otherwise a non-commercial dissolution simulation platform. Two options are available in SIMDISSO^{TM} to define bulk concentration: cell and NPV. The NPV option has a local fluid domain volume extending to a distance of one radius from the particle surface. If the system is defined as a closed system, as it was for this work, media recirculates from the cell into the reservoir and from the reservoir into the cell if the cell volume is defined as bulk volume (Fig. 2). If the NPV option is enabled, media flows directly from the reservoir into the NPV, reflecting the continuous input to the dissolution region of the cell of more dilute solution from the reservoir, and then the mass released is transported back into the cell, which is assumed to be ideally mixed. Finally, the new cell concentration is the inlet to the reservoir concentration in the next timestep as, while dissolution is a continuous process, dissolution is simulated over a series of timesteps with each timestep simulating a (user-defined) fraction of a second.

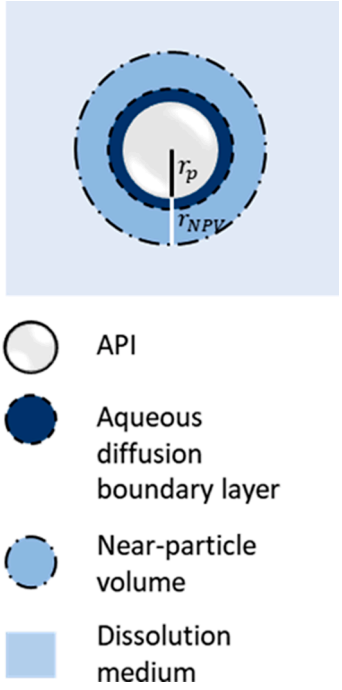

Fig. 1. Illustration of spherical API particle with radius r_p, near-particle volume (NPV), with radius extending a distance of one particle radius from the particle surface into the dissolution medium, aqueous diffusion boundary and dissolution medium surrounding each particle in the dissolution media.

In the paddle apparatus, unless poor mixing is detected, it is reasonable to consider a homogeneous distribution of drug particles in the dissolution medium and therefore using vessel volume as bulk volume could result in an accurate simulated dissolution profile (McCarthy et al., 2004). Nevertheless, there can be some regions of low velocity in the bottom of the vessel (Baxter et al., 2005; Kukura et al., 2004) or some particular situations where the mixing is poor (Kukura et al., 2003), for example, when viscous media is used (Higuchi et al., 2015), that could benefit from a more local volume to the particle when aiming for a more accurate simulated dissolution profile. In the simulations in the current work, the two options available for bulk concentration calculation are explored, the whole vessel volume or NPV with recirculation between them when the latter is enabled (Fig. 2).

The effect of bulk volume is depicted in Fig. 3. As the volume available for the particle to dissolve increases, by switching from NPV to cell or vessel volume (cases A and B), the dissolution rate is expected to increase due to bulk concentration reduction. In general, when working closer to saturation conditions – greater mass, lower solubility and lower fluid velocity -, it is hypothesised that having an NPV will be more impactful on the dissolution rate simulation. The change in NPV concentration over time is a function of fluid velocity, flow-through cell cross-sectional area and the ratio between bulk volume and cell or vessel volume.

In terms of particle diameter, either an average or median experimentally obtained particle size, or different particle size bins to capture particle size distribution, can be used. The latter is expected to increase the accuracy of the prediction (Hintz and Johnson, 1989; Okazaki et al., 2008). In that case, each particle size bin dissolves at a rate based on its mass and surface area, but against a concentration gradient which contains a contribution from every bin. Apart from the combined contribution to the concentration gradient, any other interactions between particles in the experimental setup are not currently considered in the simulations. As the particles dissolve, a new particle size is calculated for each time step, which will impact surface area and particle velocity, ultimately affecting the mass transfer rate at the next timestep.

The dissolution rate will also be affected by particle motion. Particle motion for a moving particle in the flow-through apparatus is pulsing due to the pulsing flow of the fluid, but more complex velocity patterns have been found (D'Arcy and Persoons, 2011). Two possibilities are available in SIMDISSO^{TM}, namely enabling or disabling particle motion. When particle motion is disabled, particles are exposed only to fluid velocity whereas when particle motion is enabled, particles are exposed to a relative velocity, which is the difference between fluid and particle velocity.

Ibuprofen was used as a sample drug in the current work. It is a class II drug according to the Biopharmaceutical Classification System (BCS) (Potthast et al., 2005) and class I according to the Developability Classification System (DCS) (Butler and Dressman, 2010), due to its high permeability (Loisios-Konstantinidis et al., 2020) and pH-dependent solubility, low at pH 1.2 and 4.5 and high at pH 6.8.

The aim of this paper is to assess the predictive ability of SIMDISSO^{TM} when (1) using the near-particle volume (NPV), which extends from the particle surface to a distance of one particle radius, versus the flow-through apparatus cell volume or the paddle apparatus vessel volume as the relevant instantaneous volume for the dissolution of two drug loadings in a closed system, (2) assessing the effect of inputting particle size distribution instead of a median particle size and (3) exploring the effect of enabling or disabling particle motion, in two media and with two fluid velocity conditions. The applicability of the model is investigated by means of extracting the predicted time to 85% or 50% dissolution and comparing it to the experimental time in each of the three simulated scenarios.

2. Simulation theory

The SIMDISSO^{TM} model has been described elsewhere (D'Arcy and

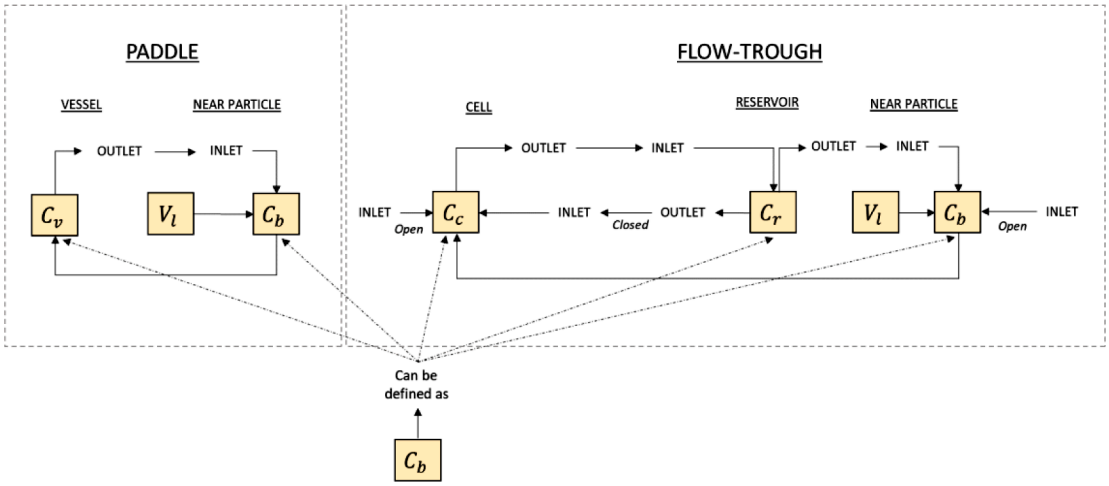

Fig. 2. Schematic definition of bulk concentration in each apparatus. C_b, bulk concentration, C_v, vessel concentration, C_c, cell concentration, C_r, reservoir concentration, V_l, near particle volume.

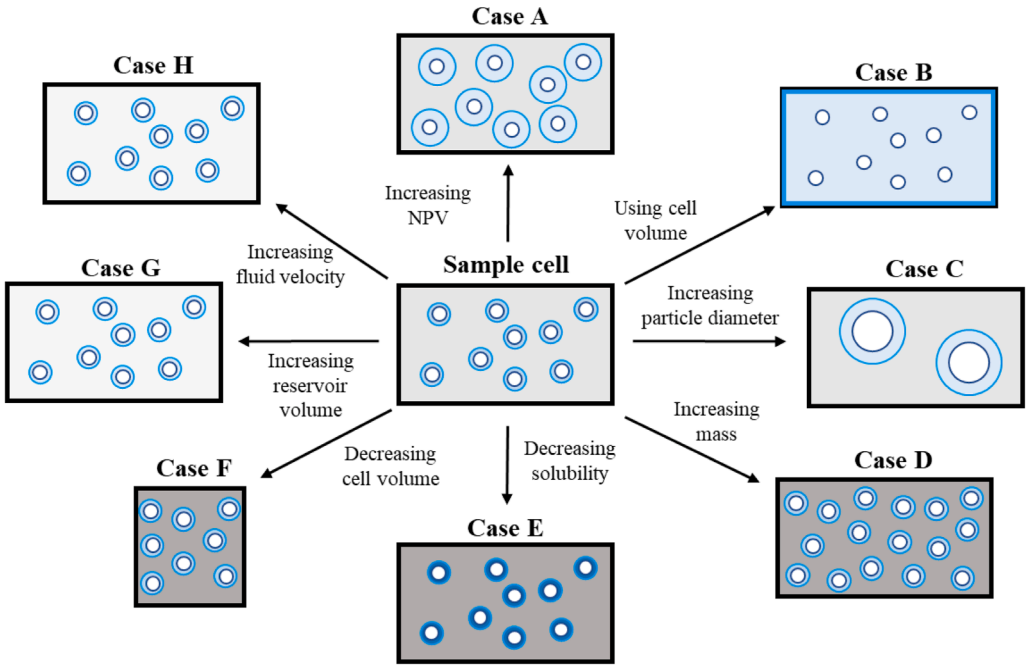

Fig. 3. Initial conditions for dissolution in a sample volume containing a mass of spherical particles (white circles) of a given diameter, solubility and diffusivity surrounded by a near-particle volume (light blue circles). Once dissolved, molecules are transported from the NPV to the total volume. The intensity of the colour reflects the degree of saturation, light blue or light grey being a dilute system and dark blue or dark grey a concentrated system.

Persoons, 2019, 2011). Briefly, it represents a lumped parameter mechanistic dissolution model which estimates a mass transfer coefficient (k) (Equation 1) for each timestep by calculating the Reynolds number (Re), Schmidt number (Sc) and Sherwood number (Sh) for a particle in a known fluid velocity field, through the Ranz-Marshall correlation (Cammarn and Sakr, 2000)(Sugano, 2008) (Equation 2) and associating it with solubility and drug surface area to predict the dissolution rate at any moment in time.

$$Sh = k(d_p)/D \tag{1}$$

$$Sh = 2 + 0.6Re^{1/2}Sc^{1/3} \tag{2}$$

where D is the diffusion coefficient and d_p is particle diameter, which can be a median particle size (MPS) or several particle diameters from a particle size distribution (PSD). In line with equations (1) and (2), the particles are assumed to be spherical and to act independently in the dissolution environment. These assumptions can result in an underestimation of available surface area due to the low surface:volume ratio of a sphere, and conversely an overestimation of surface area as particle aggregation effects are not captured in the simulation. Nonetheless, in addition to being a common approach to mechanistic mass transfer simulations, the assumption of sphericity facilitates particle motion simulations and thus hydrodynamic effects.

One of the features of SIMDISSO^{TM} is that it can capture the hydrodynamic effects of the *in vitro* system used by means of incorporating a relative velocity term in Re. If particle motion is disabled, the relative velocity becomes equal to the fluid velocity. SIMDISSO^{TM} is a reduced-order model and only one time-dependent fluid velocity parameter is included, which represents a characteristic fluid velocity in the dissolution cell. When particle motion is enabled, it is calculated for each

timestep as the sum of the forces acting over the particle divided by the apparent mass of the particle. By simulating the effect of these forces, the change in particle velocity with time can be estimated and the new particle velocity can be used as an input for the next timestep.

3. Experimental methods

3.1. Solubility study

120 mg and 30 mg of ibuprofen (Glentham Life Sciences Ltd) were added to 10 ml of 0.2M phosphate buffer pH 6.8 or 10 ml of 0.1M HCl, respectively, following the shake flask method (Alsenz and Kansy, 2007). Tests (n=3) were carried out in parallel in medium containing 0.003% w/v Tween 20. The solutions were placed in a shaking water bath at 37°C and 100 rpm (Precision Reciprocal Shaking Bath Model 25). Samples were withdrawn at 1, 5, 24, 48 and 72 hours, filtered through a 0.45 μm PVDF filter (UltraCruz™, Santa Cruz Biotechnology, Inc.) and analysed at 222 nm in a UV-Vis spectrophotometer (PharmaSpec 1700, Shimadzu) (n =3).

3.2. Optical microscopy

Ibuprofen powder was visualized under an Olympus BX53 optical microscope (Mason Technologies) with a 20x magnification.

3.3. Particle size analysis

Ibuprofen particle size determination (n=3) was carried out using a Mastersizer 3000 (Malvern Analytics) in wet mode with the Hydro MV accessory and a measurement time of 10 seconds. A saturated solution of ibuprofen in phosphate buffer with 0.003% w/v Tween 20 was used as the dispersant. The refraction index of the particle was 1.52 and the absorption index was 0.010. A PSD was calculated by generating five fractions each containing 20% of the total volume of particles. The median size was calculated for each fraction. To allocate bins for PSD, 20% of the total mass was allocated to each median size.

3.4. Surface area analysis

Samples (n=2) were degassed at 50°C overnight under nitrogen gas flow using a SmartPrep degasser (Micromeritics). Subsequently, specific surface area was measured in a Gemini VI analyser (Micromeritics) following the Brunauer-Emmett-Teller (BET) method by determining the amount of nitrogen adsorbed to the ibuprofen crystals' surface at the relative pressures of 0.05, 0.1, 0.15, 0.2, 0.25 and 0.3.

3.5. Dissolution tests

Dissolution tests were carried out in triplicate in a SOTAX CE7 smart flow-through apparatus and an Agilent 708-DS paddle apparatus.

3.5.1. Media preparation

3.5.1.1. Phosphate buffer. 0.2M phosphate buffer was prepared and degassed according to the United States Pharmacopeia (USP) (Buffer Solutions, (USP) 2021). 6.8 g of potassium phosphate monobasic (Honeywell Fluka®) and 0.003% w/v Tween 20 (Sigma-Aldrich) were added to 112 ml of a 0.2M NaOH solution and the volume was made up to 1L of deionised water. The pH of the buffer was 6.80±0.02.

3.5.1.2. 0.1M HCl. 1000 ml of 0.1M HCl were prepared by diluting 8.3 ml of 37% HCl (Honeywell Fluka®) and 0.003% w/v Tween 20 in deionised water.

3.5.2. Dissolution tests in the flow-through apparatus

Two average linear fluid velocities were achieved by combining a flow rate of 16 ml/min and a cell diameter of 12 mm (2.35 mm/s; fast velocity) or a flow rate of 8 ml/min and a cell diameter of 22.6 mm (0.33 mm/s; low velocity) in a closed system. The reservoir volume was 200 ml.

The ibuprofen mass was placed in the cell on top of the glass beads, which filled the conical part of each cell. Each glass bead was 1 mm in diameter and 2.8 mg. The mass used was 0.947 g for the 12 mm diameter cell and 6.128 g for the 22.6 mm diameter cell. A GF/D glass microfiber filter (GE Healthcare Life Sciences Whatman™) was placed on top of the cell to retain undissolved particles. 2 ml samples were taken at 2, 4, 8, 15, 30, 45, 60, 90 and 120 minutes for phosphate buffer and 10, 20, 40, 60, 90, 150, 210 and 270 minutes for HCl. Samples were replaced with fresh medium at 37°C after each sampling point.

3.5.3. Dissolution tests in the paddle apparatus

The ibuprofen mass was placed inside a Vcaps® HPMC capsule size 3, kindly donated by Lonza, and a sinker and added to 500 ml of dissolution medium. Time zero was set as the time when the first capsule was observed to rupture.

3 ml samples were taken at 2, 4, 6, 8, 10, 15, 30, 45 and 60 minutes for phosphate buffer and at 10, 20, 40, 60, 90, 120, 180, 240 and 300 minutes for HCl. The sampling probe was only introduced at the moment of sampling to minimize alteration of hydrodynamics in the vessel (Chapter 1094, (USP) 2021). Samples were filtered using PTFE filters (0.45 μm, Fisherbrand) and the first millilitre was discarded. Samples were replaced with fresh medium at 37°C after each sampling point.

3.5.4. Analysis of the samples

All samples were analysed by UV-Vis spectrophotometry (PharmaSpec 1700, Shimadzu) at either 222 nm for 5 mg tests or 264 nm for 50 mg tests, due to the higher sensitivity at 222 nm and reduced need for dilution at 264 nm.

3.6. Computational methods

3.6.1. Input parameters for the flow-through apparatus

Simulations in the flow-through apparatus were performed with either (1) 5 or 50 mg, (2) pH 6.8 phosphate buffer or 0.1M HCl and (3) 2.35 mm/s and 0.33 mm/s as average linear fluid velocities in a pulsing flow field. Inputs are presented in Table 1.

The cell volume was calculated based on 30 mm of the upper cylindrical part of the cell and not including the conical section containing the glass beads, nor regions in the upper cell where the diameter changes, as a constant diameter is required to calculate the instantaneous linear velocity in the cell and the relative particle velocity.

The cell volume, the experimentally determined median particle size (MPS) and particle motion enabled were inputs for the initial reference simulation. Simulations were assessed for improved predictability by (1) using an NPV (2) inputting a PSD and (3) disabling particle motion.

Particle size, density and phosphate buffer solubility inputs were experimentally determined. In HCl (pH 1.5), the theoretical solubility value obtained using equation (3) (D'Arcy and Persoons, 2011;(Healy and Corrigan, 1992)) was used in the simulations (0.064 mg/ml)

$$Solubility\ (mg\,/\,ml) = 0.064\left(1 + 10^{pH-4.39}\right) \quad (3)$$

Fluid density and simulation time were media-dependent. Particle density is an estimate from measurement results described in literature (D'Arcy and Persoons, 2011). The flow profile was set to be pulsating with a pump frequency of 2 Hz (Chapter 711, (USP) 2021) and gravity was enabled as it is relevant to the direction of the flow profile in the vertical flow-through cell (D'Arcy et al., 2011).

Table 1
Experimentally determined (*) and literature extracted (†) inputs to SIMDISSO dissolution simulation code. ρ_p, particle density, D, diffusion coefficient, μ_f, fluid viscosity, V_r, reservoir volume, m_0, mass, d_p, particle diameter, U_p, particle velocity, U_f, fluid velocity, C_b, bulk concentration, C_s, solubility, ρ_f, fluid density.

Constant inputs			Variable inputs				
	Flow-through	Paddle		Flow-through		Paddle	
† ρ_p (g/cm^3)[12]	1.018		m_0 (g)	0.005, 0.050		0.003, 0.050	
			d_p (mm)	0.160, PSD		0.160, PSD	
			Number of Size bins	1, 5		1, 5	
† D (m^2/s) [13]	8*10^{-10}		U_p	Enabled, Disabled		Enabled	
			† Cell diameter (mm) [13]	0.0226	0.012	-	
Particle shape	Spherical		† Flow rate (ml/min)[13]	8	16	-	
			† U_f (m/s) [28,29]	-		0.0766 (50 rpm), 0.1476 (100 rpm)	
† μ_f (mPa s)[13]	0.7		C_b calc.	NPV, Cell		NPV, Cell	
Pumping mode	Pulsating	Steady	**Medium properties and solubility**				
				Flow-through		Paddle	
V_r (ml)	200	500		Phosphate buffer	0.1M HCl	Phosphate buffer	0.1M HCl
			* C_s (mg/cm^3)[12]	3.5	0.064	3.5	0.064
Gravity (m/s^2)	9.81	Disabled	* ρ_f (g/cm^3)	1.009	1.006	1.009	1.006
† Pump frequency (Hz)[1]	2	-	Simulation time (min)	90	300	45	300
Type of system	Closed		Time steps (s)	0.004	0.004	0.004	0.004

3.6.2. Particle motion simulations

10-seconds simulations were run to interpret the initial effect of disabling or enabling particle motion in the flow-through apparatus.

Two average linear fluid velocities were used: 0.33 mm/s and 2.35 mm/s, to match the experimental flow rates and cell diameters. Other inputs were 5 mg mass, 160 μm MPS, 200 ml reservoir volume, 0.064 mg/ml solubility and 1.006 g/cm^3 fluid density. The constant inputs are as described in Table 1. Particle motion and gravity were enabled. The results presented here are calculated in 0.1M HCl, but the same results were obtained for phosphate buffer, due to an almost equal density, same fluid velocity, same particle properties and minimal dissolution over 10 seconds.

3.6.3. Input parameters for the paddle apparatus

Inputs to the simulations in the paddle apparatus are shown in Table 1. The fluid pumping mode was set to steady as there is no pulsating option for the paddle apparatus, particle motion was enabled and gravity disabled as tangential velocity is the main velocity component in the paddle apparatus (McCarthy et al., 2003; Todaro et al., 2017), and fluid velocity data were extracted from literature (Bai et al., 2011, 2007) to be equivalent to a rotational speed of 50 rpm or 100 rpm.

3.7. Statistical analysis

All experimental measurements were carried out in triplicate apart from surface area analysis, and presented as the mean value ± standard deviation. Two-sided t-tests were carried out to determine whether there was a statistically significant difference between the solubilities of the dissolution media with and without surfactant. A confidence level of 95% was selected.

The time to 85% dissolution in phosphate buffer (t85) and 50% dissolution in HCl (t50) was directly extracted from simulation outputs and experimental profiles.

For profiles exploring the effect of PSD, the experimental dissolution profiles were compared to the simulated MPS and PSD profiles for each time point by calculating the percentage predicted error (PE%) and the root mean square error (RMSE) to illustrate predictability over the whole profile:

$$PE\% = \frac{|Simulated\ value - Experimental\ value|}{Experimental\ value} * 100 \quad (4)$$

$$RMSE = \sqrt{\frac{1}{n}\sum_{i=1}^{n}(Simulated\ value - Experimental\ value)^2} \quad (5)$$

4. Results

4.1. Solubility study

The solubility of ibuprofen in phosphate buffer with and without Tween 20, was 3.5±0.5 mg/ml and 4.1±0.3 mg/ml after 48 hours of incubation. The pH values of the saturated solutions were 6.05 and 6.10, respectively, which is in accordance with the surface pH of ibuprofen in phosphate buffer reported in literature (Cristofoletti and Dressman, 2016). The solubility values with and without surfactant were not statistically significantly different, therefore the value of 3.5 mg/ml was used in the simulations of dissolution in phosphate buffer with Tween 0.003% w/v. Solubility in 0.1M HCl with and without Tween 20, was 0.063±0.016 mg/ml and 0.066 ±0.012 mg/ml after 24 hours of incubation, which was in agreement with intrinsic solubility values presented in literature (Krieg et al., 2015; Levis et al., 2003). Therefore, the calculated value (eq 3) of 0.064 mg/ml was used as input for the simulation.

4.2. Particle size analysis

The experimental d50 value was 160±0.197 μm. The particle sizes of the each of the PSD bins were 12.7 μm, 81.2 μm, 135.5 μm, 240 μm and 551 μm.

4.3. Dissolution tests in flow-through apparatus

4.3.1. Cell volume vs near-particle volume

The experimental and simulated dissolution profiles of 5 mg of ibuprofen at two average fluid velocities, 2.35 mm/s and 0.33 mm/s, in phosphate buffer and 0.1M HCl were compared (Fig. 4). Simulated results were obtained using an MPS and enabled particle motion and either the cell volume or the NPV.

The experimental dissolution rate of 5 mg of ibuprofen in phosphate buffer would be considered rapid (85% within 30 minutes) by the FDA guidance for BCS class I or III drugs in the paddle apparatus at 50 rpm ((FDA, 2017)), which was expected due to its high solubility at pH 6.8. In 0.1M HCl, after 270 minutes, only 73% was dissolved in the fast fluid velocity test and 57% in the low fluid velocity test, due to the low solubility of ibuprofen in HCl and the lack of sink conditions, as has been reported for other drugs (Van der Vossen et al., 2019).

The experimental dissolution rates decreased in a lower fluid velocity environment in both media. In phosphate buffer, the NPV and cell options predicted very rapid dissolution, however use of the NPV suggested velocity effects on dissolution which were not apparent in the

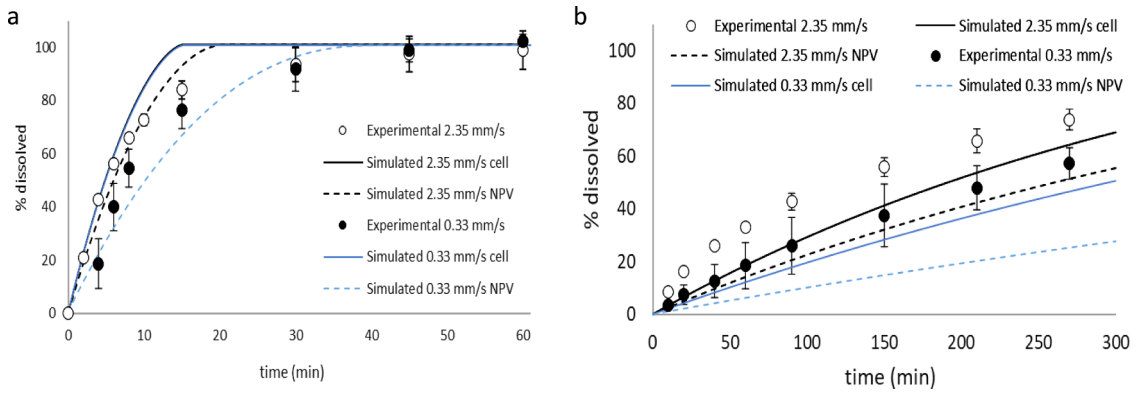

Fig. 4. Experimental dissolution profiles of 5 mg of 160 μm median diameter ibuprofen particles in 200 ml of (a) pH 6.8 phosphate buffer or (b) 0.1M HCl, with 0.003% w/v Tween 20 at 37°C in the flow-through apparatus at two average linear fluid velocities: 2.35 mm/s (white circles) and 0.33 mm/s (black circles). Simulated profiles were obtained with an MPS and particle motion enabled and either cell volume (solid lines) or a near-particle volume (dashed lines) for 2.35 mm/s (black) and 0.33 mm/s (blue).

simulation using the cell option as the bulk volume. Furthermore, the NPV option was better at predicting t85 than the cell volume option, in both velocities (Table 2). In 0.1M HCl, the NPV underpredicted the dissolution rate in both fluid velocities and did not increase the t50 predictive ability. The underprediction from all simulations in 0.1M HCl (Fig. 4) could be attributed to the assumption of sphericity by the model, whereas the majority of the particles are needle-shaped, as shown by optical microscopy (Fig. 5). However, while the calculated surface area for the 5 mg sample using the MPS (1.8 cm^2) was lower than the measured surface area (5.3 cm^2), the calculated surface area using the PSD (6.15 cm^2) compared well with the measured area. Therefore the underestimation of surface area resulting from the assumption of spherical particles is likely to have a minor impact in the current work.

The effect of fluid velocity on dissolution rate is due to the local medium being more concentrated in each timestep because of a reduced mass transport rate away from the dissolving surface affecting the local concentration gradient and slowing down the dissolution process. An effect of the flow rate on dissolution rates has been described before (D'Arcy and Persoons, 2011), possibly due to a better dispersal of the particles as the flow rate increases as well as the effect on local concentration gradients.

Therefore, an NPV seemed more accurate in predicting dissolution in high solubility than low solubility conditions, although other simulation parameters, such as particle size and particle motion definition can affect the accuracy of the prediction, as will be discussed.

4.3.2. *Particle size distribution vs median particle size*

The simulations were run with an NPV, particle motion enabled and either an MPS or a PSD. Although the shape of the 5 mg dissolution profile in phosphate buffer resembled the experimental results more closely than when an MPS was used in both velocities, (Fig. 6a), the predictive error and RMSE were larger for the simulations using a PSD (Fig. 7a). This is due to the fast simulated dissolution at early timepoints from the contribution of the small particles (12.7 μm) and the slower simulated dissolution at later timepoints due to the dissolution of larger particles (551 μm).

Table 2
Time to 85% or 50% dissolution (min) in the flow-through apparatus with a constant 200 ml reservoir volume and gravity enabled. Some of the simulations in the low solubility environment (0.1M HCl + 0.003% w/v Tween 20, represented by a solubility of 0.0064 mg/ml) did not reach 50% dissolved in 300 min.

Variables							Time to 85% dissolution in flow-through apparatus	
Test ID	Solubility (mg/ml)	Mass (mg)	Velocity (mm/s)	Bulk volume	Particle size (μm)	Particle motion	Simulated	Experimental
1	3.5	5	2.35	Cell	MPS	On	9.99	16.92±5.51
2	3.5	5	2.35	NPV	MPS	On	12.55	
3	3.5	5	2.35	NPV	PSD	On	18.03	
4	3.5	5	2.35	NPV	PSD	Off	16.11	
5	3.5	5	0.33	Cell	MPS	On	10.09	22.43±4.36
6	3.5	5	0.33	NPV	MPS	On	22.13	
7	3.5	5	0.33	NPV	PSD	On	22.34	
8	3.5	5	0.33	NPV	PSD	Off	30.53	
9	3.5	50	2.35	Cell	MPS	On	10.98	40.89±1.38
10	3.5	50	2.35	NPV	MPS	On	16.05	
11	3.5	50	2.35	NPV	PSD	On	19.98	
12	3.5	50	2.35	NPV	PSD	Off	18.23	
13	3.5	50	0.33	Cell	MPS	On	11.53	69.65±7.01
14	3.5	50	0.33	NPV	MPS	On	37.19	
15	3.5	50	0.33	NPV	PSD	On	30.58	
16	3.5	50	0.33	NPV	PSD	Off	38.30	
							Time to 50% dissolution in flow-through apparatus	
17	0.064	5	2.35	Cell	MPS	On	282.68	131.01±16.85
18	0.064	5	2.35	NPV	MPS	On	>300	
19	0.064	5	2.35	NPV	PSD	On	223.42	
20	0.064	5	2.35	NPV	PSD	Off	174.50	
21	0.064	5	0.33	Cell	MPS	On	284.30	219.35±44.84
22	0.064	5	0.33	NPV	MPS	On	>300	
23	0.064	5	0.33	NPV	PSD	On	>300	
24	0.064	5	0.33	NPV	PSD	Off	>300	

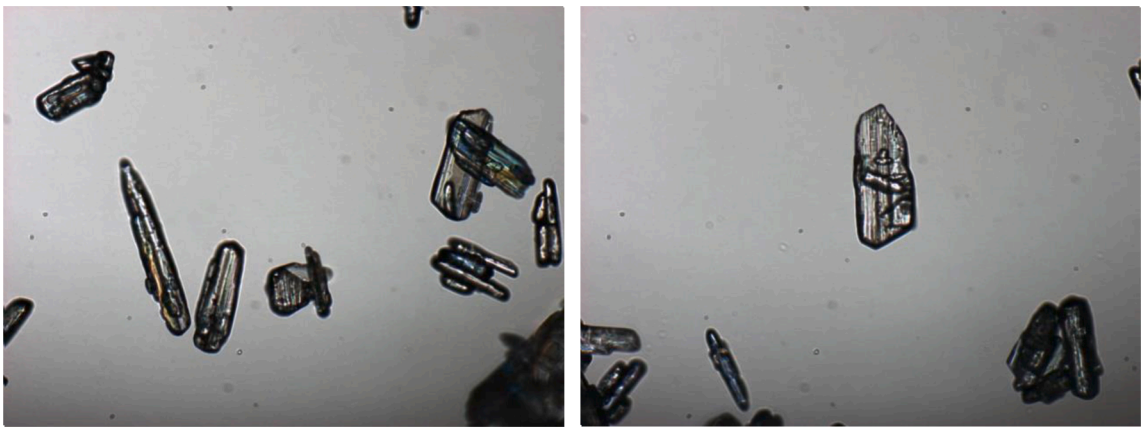

Fig. 5. Ibuprofen crystals visualized under Olympus BX53 optical microscope with a magnification of x20.

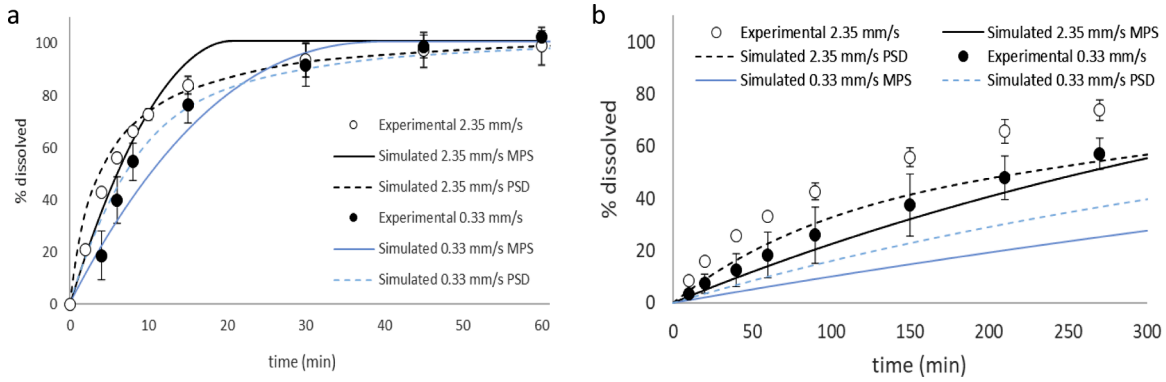

Fig. 6. Experimental dissolution profiles of 5 mg of 160 μm median diameter ibuprofen particles in 200 ml of (a) pH 6.8 phosphate buffer or (b) 0.1M HCl, with 0.003% w/v Tween 20 at 37°C in the flow-through apparatus at two average linear fluid velocities: 2.35 mm/s (white circles) and 0.33 mm/s (black circles). Simulated profiles were obtained with a near-particle volume and particle motion enabled and either an MPS (solid lines) or a PSD (dashed lines) for 2.35 mm/s (black) and 0.33 mm/s (blue).

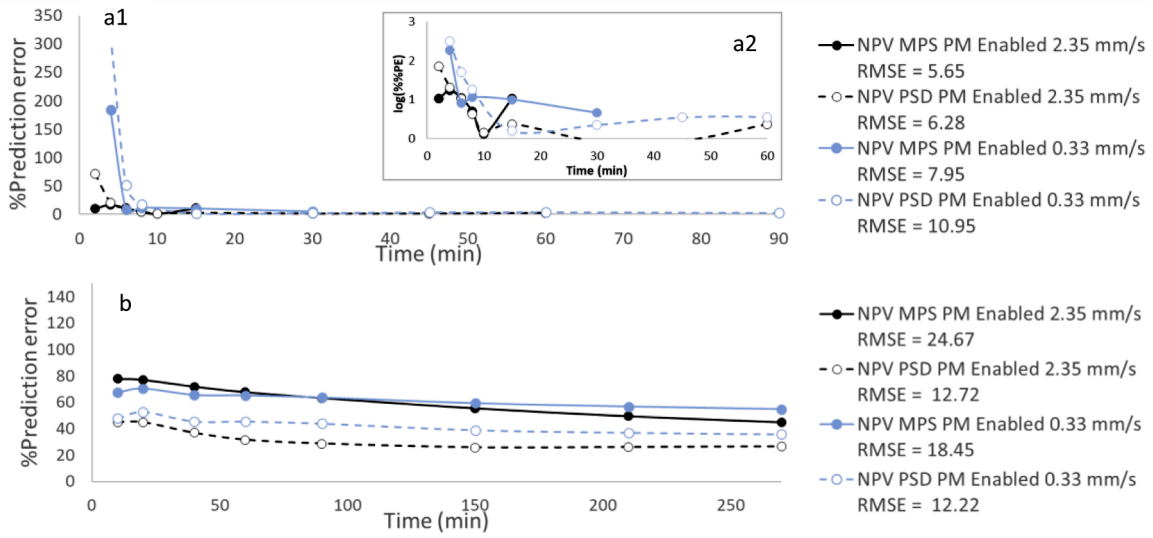

Fig. 7. Percentage predicted error (a1) and log percentage predicted error (PE) (a2) vs time profiles and RMSE values of 5 mg of 160 μm median diameter ibuprofen particles in 200 ml of (a) pH 6.8 phosphate buffer or (b) 0.1M HCl with 0.003% w/v Tween 20 at 37°C in the flow-through apparatus at two average linear fluid velocities, 2.35 mm/s or 0.33 mm/s. Simulated results were obtained with a near-particle volume (NPV), particle motion (PM) enabled and either a median particle size (MPS) or a particle size distribution (PSD).

Moreover, there was a particularly high predictive error for early timepoints when a PSD was used in the phosphate buffer medium, especially in the lower velocity flow field. This could be due to the hydrophobic nature of the ibuprofen particles making them prone to aggregation and therefore behaving as bigger particles at the beginning of the test, even though a small amount of surfactant was used to promote dispersal. An aggregation effect could be considered more likely in the low velocity flow field. Therefore, a PSD could be more useful for drugs not as prone to aggregation as ibuprofen (D'Arcy and Persoons, 2011). However, it was as accurate as an MPS when predicting t85 in the low velocity environment and even more accurate than an MPS in fast fluid velocity (Table 2).

In the low solubility media, 0.1M HCl, a PSD increased the prediction accuracy, reducing the RMSE and predictive error to a similar extent in both velocities (Figs. 6b and 7b). It increased the ability of the simulation to predict the t50 in a fast fluid velocity environment, even though the observed time was still exceeded by approximately 92 minutes (Table 2).

Overall, PSD improved the predictive accuracy in the low solubility environment, but a notable underprediction was still observed.

4.3.3. Particle motion enabled vs disabled

Preliminary particle motion simulation results are shown in Fig. 8. Both velocities present a semi-sinusoidal profile due to the pulsating flow with which the media enters the dissolution cell. Fluid velocities fluctuated between zero and positive values, as defined by the velocity input in the code, with two pulses per second. Particle velocity fluctuated between positive and negative values, which represent upward flow and downward flow, respectively, but the magnitude of the positive values was larger, suggesting particles would move to the top of the cell and be held there at initial stages of dissolution until small enough to move with the fluid. Therefore, these results suggest that particle motion should be disabled, at least during the first instances of dissolution. In the light of these results, simulations were run with disabled particle motion in both media.

In the case of phosphate buffer, the results were similar when disabling and enabling particle motion (Fig. 9), and within or very close to the error bars for the 5 mg profile, therefore the usefulness of disabling particle motion was not proven in that particular situation (Fig. 9a).

With respect to the predictive ability of the simulation in phosphate buffer, it gave an accurate prediction of t85 in a fast fluid velocity media, but so did the options with particle motion enabled and an NPV, and in the low fluid velocity situation it predicted a larger t85 than observed (Table 2).

In the case of 0.1M HCl, disabling particle motion in a fast fluid velocity situation led to the most accurate prediction of the four options and the closest t50 to the observed, but it resulted in an almost superimposable profile as that generated when particle motion was enabled in the case of a low fluid velocity (Fig. 9b). This is because the difference between maximum initial relative velocity (0.225 mm/s) and maximum initial fluid velocity (1.033 mm/s) was very small in this scenario, therefore the velocity that the particle is exposed to is similar when particle motion is enabled or disabled. In the case of a higher fluid velocity, when the particle is exposed to fluid velocity only (maximum 7.398 mm/s) – that is, when particle motion is disabled – this is of a notably larger magnitude than the relative velocity it is exposed to when particle motion is enabled (0.235 mm/s) (Fig. 8), leading to a faster dissolution rate in the former case.

Therefore, disabling particle motion only slightly increased the predictive ability in the low solubility-fast velocity conditions simulated in the current work.

4.3.4. Predictive ability of the simulation with different drug loadings

All simulation options predicted the dissolution of 5 mg of ibuprofen in phosphate buffer in the flow-through apparatus at both velocities reasonably well whereas there was a large overprediction for a mass of 50 mg (Fig. 10), especially for the fast velocity environment (Fig. 10a). Even inputting a PSD, with and without particle motion enabled, did not improve the predictions for a mass of 50 mg, compared to inputting an MPS.

Furthermore, all predicted t85 values were lower than the experimental times obtained (Table 2). This overprediction of the dissolution rate was previously observed with a mass of 10 mg in the flow-through apparatus when clumping was suspected (D'Arcy and Persoons, 2011). The lower predicted t85 values in the current work could be due to visible clumping which was observed to occur in the experimental test, which reduces the surface area exposed to the medium and therefore the dissolution rate. This is not captured by the simulation, which assumes individual spherical particles that do not interact. To ensure particle dispersal a small amount of surfactant was used in the medium, namely 0.003% w/v Tween 20. This was successful in dispersing the particles without affecting solubility to a great extent when a small mass of ibuprofen was used, but clumping was still visible for the bigger mass of 50 mg. Furthermore, the time to wet the particles at the beginning of the test, resulting in a reduced initial effective surface area for dissolution,

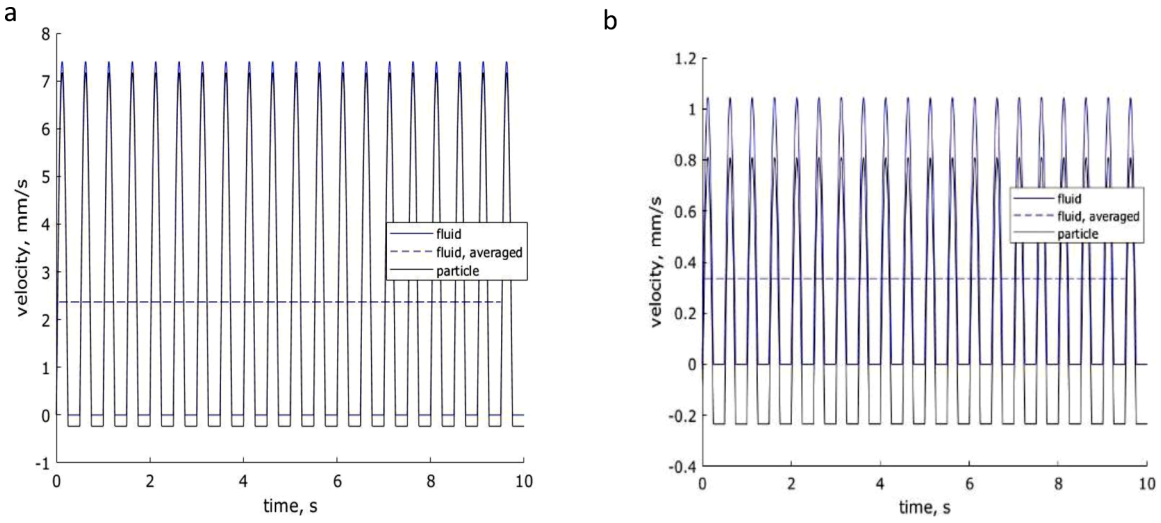

Fig. 8. Particle motion simulations for 5 mg of 160 μm diameter ibuprofen particles in 200ml of 0.1M HCl at 37°C in the flow-through apparatus with (a) a flow rate of 16 ml/min and a cell diameter of 12 mm or (b) a flow rate of 8 ml/min and a cell diameter of 22.6 mm.

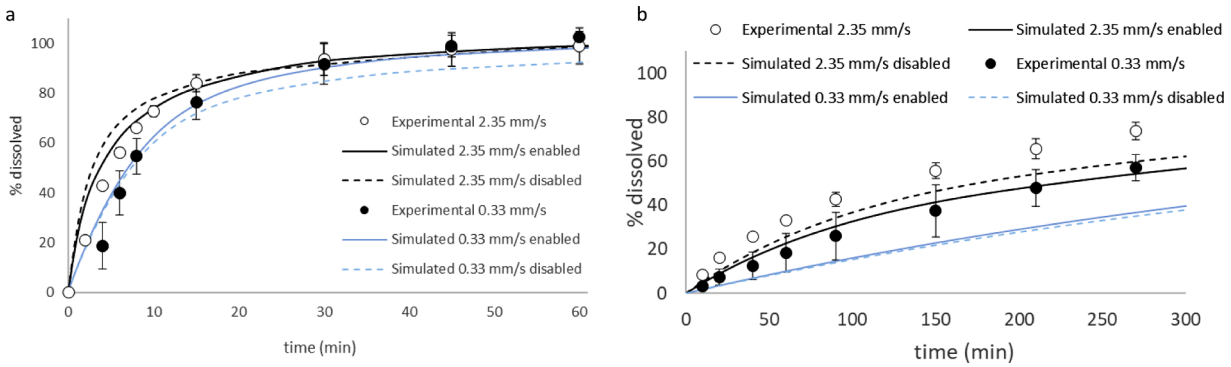

Fig. 9. Experimental dissolution profiles of 5 mg of 160 μm median diameter ibuprofen particles in 200 ml of (a) pH 6.8 phosphate buffer or (b) 0.1M HCl, with 0.003% w/v Tween 20 at 37°C in the flow-through apparatus at two average linear fluid velocities: 2.35 mm/s (white circles) and 0.33 mm/s (black circles). Simulated profiles were obtained with a particle size distribution, near-particle volume and particle motion enabled (solid lines) or disabled (dashed lines) for 2.35 mm/s (black) and 0.33 mm/s (blue).

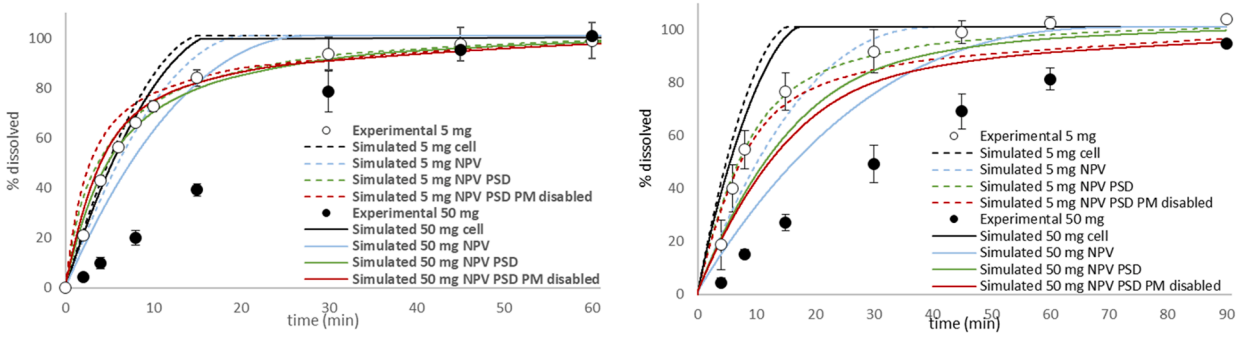

Fig. 10. Experimental (exp) dissolution profiles of 5 mg (white circles) and 50 mg (black circles) of 160 μm diameter ibuprofen particles in 200 mL of pH 6.8 phosphate buffer with 0.003% w/v Tween 20 at 37°C in the flow-through apparatus at two average linear fluid velocities of (a) 2.35 mm/s and (b) 0.33 mm/s. Simulated (sim) profiles were obtained for 5 mg (dashed lines) and 50 mg (solid lines) with an MPS, particle motion enabled and cell volume (black); an MPS, particle motion enabled and near-particle volume (blue); a PSD, particle motion enabled and near-particle volume (green); a PSD, particle motion disabled and near-particle volume (red).

may be influencing the overprediction. Wetting issues have been observed previously in the dissolution of ibuprofen API (Cristofoletti and Dressman, 2017). Therefore, the effect of mass is important in terms of inputting an accurate particle size in the simulation.

In addition to clumping, the saturation with a higher mass can affect the local instantaneous concentration. When using the cell volume option in the simulation, combined with an MPS and enabled particle motion, no difference in dissolution rate was predicted between both masses in phosphate buffer at both velocities. This can be attributed to a very low bulk concentration in the whole reservoir volume of 200 ml entering cell volume and affecting cell concentration. When an NPV was input in the simulations instead, and the rest of the inputs where maintained, the simulations predicted a difference in the dissolution rate of the two masses in phosphate buffer, and this difference was larger for a low fluid velocity. This was due to a smaller instantaneous volume available for the particles to dissolve, and therefore a reduction in the magnitude of the gradient driving dissolution.

When working under sink conditions, as defined by reservoir volume concentration, this observed difference in dissolution between masses is not expected as bulk concentration is assumed to be negligible, however this assumption may be too simplistic for dissolution conditions with low fluid velocity, where the amount of drug transported from the cell into the reservoir is smaller per timestep. Therefore, the fluid local to the dissolving particle might become more concentrated and theoretical sink conditions may not be occurring at all instances in practice.

Overall, even though there was an overprediction in simulated dissolution rates, the relative difference between dissolution rates in each flow field, for a mass of 50 mg, was somewhat captured by the NPV-PSD simulations (70% experimental difference vs 55% simulated difference).

4.4. Dissolution tests in the paddle apparatus

Four tests in the paddle apparatus are presented in Fig. 11: 50 mg in phosphate buffer at (1) 100 rpm and (2) 50 rpm and 3 mg in HCl at (3) 100 rpm and (4) 50 rpm. Again, dissolution in phosphate buffer was rapid (85% within 30 minutes) and, in contrast to the flow-through apparatus, 100% dissolved was observed in the experimental 0.1M HCl test at 100 rpm due to presence of sink conditions.

There was an experimental difference in the dissolution profiles between operating at 50 and 100 rpm in both media that was not reflected in the simulated profiles, where both profiles were superimposable. This can be due to better dispersion at 100 rpm and observed sedimentation at 50 rpm which would result in the particles being exposed to very different velocities in each case. Dissolution in phosphate buffer was incomplete after one hour, but it was sufficient to determine t85. Furthermore notable variability was observed, especially at 50 rpm (Table 3). The observed sedimented undissolved material at the 1 hr time point is likely due to poor initial wetting and subsequent poor dispersal of ibuprofen particles in the low velocity region at the centre of the vessel base. Whereas it is also possible that the relatively high concentration of buffer salts used resulted in the formation and precipitation of sodium or potassium salts of ibuprofen during the dissolution test (Cristofoletti and Dressman, 2017), similar undissolved material was not noted in the flow through apparatus tests, suggesting an impact from system hydrodynamics.

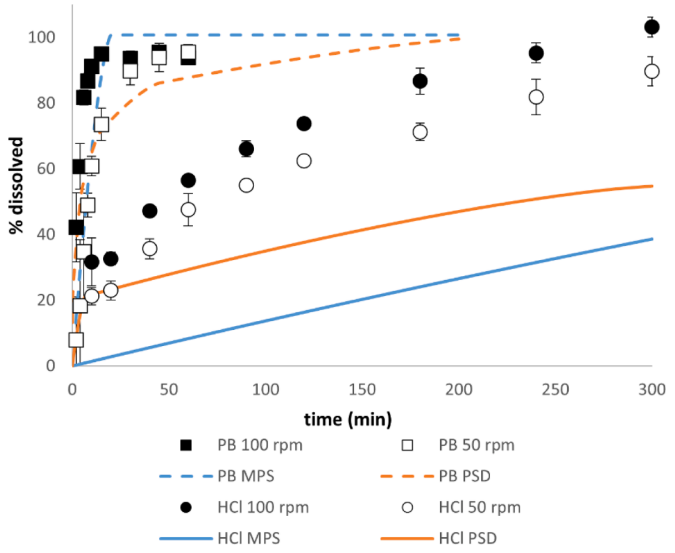

Fig. 11. Experimental dissolution profiles of 50 mg of 160 μm median diameter ibuprofen particles in 500 ml of pH 6.8 phosphate buffer with 0.003% w/v Tween 20 (squares) and 3 mg in 500 ml 0.1M HCl with 0.003% w/v Tween 20 (circles) at 37°C in the paddle apparatus at two agitation speeds: 50 rpm (white) and 100 rpm (black). Simulated profiles were obtained with an MPS (blue) or a PSD (orange). Simulated results were obtained using a velocity of 0.1746 m/s, representing 100 rpm or 0.0766 m/s, representing 50 rpm (results were superimposable) and cell volume or near-particle volume (results were superimposable). Particle motion was enabled in all simulations.

In both media, the PSD option seemed more accurate than an MPS from the dissolution profiles in Fig. 11. However, in terms of predictions, an MPS was relatively accurate in predicting <30 minutes for t85 in phosphate buffer at a 100 rpm (predicted 14 min vs experimental 8 min), and more accurate than a PSD, due to the slow simulated dissolution of the bigger particles in later stages of dissolution (Table 3).

Neither an MPS nor a PSD were accurate in predicting the time dissolved at 50 rpm probably because the sedimentation observed during the test was not captured by the simulation, which incorporated only tangential velocity effects. Furthermore, there was no difference in using the cell volume or an NPV for either medium. This can be due to both the fluid velocity and the cross-sectional flow area, which influence how NPV concentration changes over time, being of a higher magnitude in the paddle apparatus simulations than in the flow-through apparatus.

In 0.1M HCl, a PSD simulation predicted a closer t50 when compared to an MPS (Table 3), however both t50 predictions were of a much higher magnitude than the experimental results, as can be observed by the underprediction in Fig. 11.

5. Discussion

The predictions were overall accurate for the rapid dissolution of a low mass of ibuprofen in phosphate buffer, but there was a general underprediction in 0.1M HCl. This could be due to surface area effects leading to a faster dissolution due to the discrepancy between the actual particle morphology and the assumption of spherical particles in the simulation, however in the current work the simulation using PSD suggested only a minor impact if any from the assumption of sphericity on available surface area. Conversely there was an overprediction of dissolution rate in a high mass system, likely influenced by agglomerated particles observed in the dissolution cell. The observed needle-shaped particle morphology is also likely to contribute to particle agglomeration and caking to a greater extent than would be expected from spherical particles.

In considering dissolution according to Nernst Brunner equation, flow rate will affect dissolution rate as it would impact the aqueous diffusion boundary layer thickness. In the presented model, using the Ranz-Marshall correlation, the hydrodynamic effect is captured by the Reynolds number, even without considering an NPV. However, defining bulk concentration using NPV better captured the velocity effect.

An NPV volume in the current work was defined as a spherical volume surrounding the particle, which extends a distance of one radius from the particle surface. This NPV is a hypothetical situation of a bulk volume which is smaller than the reservoir (or vessel) volume, but how this volume is defined can vary. Any multiple of radii can be input but one radius was chosen as the smallest NPV thickness that can reasonably be explored since in a static fluid, due to the asymptotic molecular diffusion effect, the Sherwood number has been demonstrated to equal 2, meaning the aqueous diffusion boundary layer (ADBL) thickness equals the particle radius (Sugano, 2008). In a moving fluid, where an Re-dependent term is included, the ADBL thickness will decrease, although due to the pulsing flow in the flow-through apparatus there can still be periods of near static fluid. Therefore, the thickness of the ADBL will not exceed the NPV thickness at any moment in time. An NPV extending one radius from the particle surface is considered to be the minimum NPV which can be explored if the dissolution media has periods of static motion. The current work represents an illustration of the effect of a reduced volume in dissolution simulations as sink conditions might be present globally but not locally, especially in the flow-through apparatus with a pulsing flow with periods of very low velocity. The results presented indicate that the concept of a more dynamic bulk concentration definition, influenced by both local and reservoir concentrations and transport between both, is potentially useful both in simulating dissolution in the flow-through apparatus and in considering the effect of flow rate, pulsation and cell size on experimental results.

A PSD increased the predictive ability of the simulations in low solubility media, but it might not always be required, as was shown in the case of a hydrophobic drug such as ibuprofen in a fast dissolution environment, pH 6.8 phosphate buffer, where use of an MPS could be considered sufficiently accurate for many applications. The measured

Table 3
Time to 85% or 50% dissolution (min) in the paddle apparatus with 500 ml reservoir volume and gravity disabled. Some of the simulations in the low solubility environment (0.1M HCl + 0.003% w/v Tween 20, represented by a solubility of 0.0064 mg/ml) did not reach 50% dissolved in 300 min.

Variables						Time to 85% dissolution in paddle apparatus		
Test ID	Solubility (mg/ml)	Mass (mg)	Velocity (rpm)	Particle size (μm)	Particle motion	NPV	Vessel volume	Experimental
1	3.5	50	50	MPS	On	14.30	14.05	**28.14±16.74**
2	3.5	50	50	PSD	On	40.70	40.55	
3	3.5	50	100	MPS	On	14.16	14.05	**8.04±6.70**
4	3.5	50	100	PSD	On	40.58	40.61	
						Time to 50% dissolution in paddle apparatus		
5	0.064	3	50	MPS	On	-	>300	**77.87±5.08**
6	0.064	3	50	PSD	On	-	230.46	
7	0.064	3	100	MPS	On	>300	>300	**44.59±5.48**
8	0.064	3	100	PSD	On	-	230.46	

PSD might also not be representative of the effective PSD in the dissolution medium.

Furthermore, it is important to characterize particle motion, as if the difference between fluid velocity and relative velocity is large, as was the case in the fast fluid velocity in 0.1M HCl, this can affect the accuracy of the prediction. SIMDISSO^{TM} takes particle motion into account but there is scope to better explore the simulation of particle motion and local volume to optimally capture the interplay between hydrodynamic effects and local concentration gradients.

Limitations and assumptions include the assumption of individually dissolving spherical particles in the simulation code used for the current work. Therefore agglomeration of hydrophobic drugs or needle-shaped particles, which were observed experimentally, are not taken into account, and the effect of non-spherical particle morphology on surface area is not captured. The particle size input also has a large influence on the simulated profiles, and particle size measurement methodology and bin allocation will affect the predicted dissolution rates. As SIMDISSO^{TM} is a reduced-order model and only one time-dependent fluid velocity parameter is included, it is not possible to include the change in internal cell diameter in the upper region of the 12 mm diameter cell. In the current work, the 12 mm diameter cell simulations were used for the high velocity conditions only, and preliminary investigations showed that the simulated dissolution rate was not notably sensitive to a change in volume when approaching the simulated cell volume. Thus, a cylindrical portion of the cell only was simulated, to reflect the highest velocity region. If simulating lower flow rates and/or lower solubilities, it is recommended that the impact of representative velocity vs. available volume in the simulation be investigated when defining the cell volume. Finally, particle density, which can impact particle motion and thus the simulated dissolution profiles, was not measured for the current work but extracted from literature, as its effect on ibuprofen dissolution simulations was previously investigated extensively by this group (D'Arcy and Persoons, 2011).

6. Conclusions

The implementation of an NPV available for the particle to dissolve in was compared with the flow-through cell volume or paddle vessel volume. The NPV was useful to predict effects of velocity differences in a high solubility media in the flow-through apparatus, accounting for the reduction in the dissolution rate as velocity is reduced. The simulation could capture two very different environments in terms of solubility for the same drug: HCl, where ibuprofen is not very soluble (0.064 mg/ml), and phosphate buffer, where ibuprofen is highly soluble (3.5 mg/ml), even though it underpredicted the dissolution rate in low solubility conditions – in both apparatuses -, especially when the NPV option was used.

In the light of these findings, it could be argued that the cell volume option resembled the experimental profiles better in 0.1M HCl in the flow-through apparatus, however this underprediction was reduced when other factors were included in the simulation, namely a PSD and disabling particle motion. Therefore, the advantage of cell over NPV cannot be ascertained without further investigation of the confounding effects of other simulation inputs, including effects of particle morphology on exposed surface area.

The PSD option served to increase the predictive ability of the simulations especially in low solubility media. In high solubility media, the accuracy of the prediction when a PSD was used suggests that in fast dissolution situations use of an MPS could result in a sufficiently accurate simulation, reducing the computational cost.

Whether to have particle motion enabled or disabled can be informed by preliminary simulations which predict particle motion in the first ten seconds of dissolution based on particle mass, particle density and fluid velocity and density. Disabling particle motion was not advantageous in a high solubility media, but it increased the predictive ability in a high velocity-low solubility scenario pointing towards the need for a good particle motion model in dissolution simulation.

Finally, the current work also presents the predictive ability of SIMDISSO^{TM} as applied to the paddle apparatus. The accuracy of the prediction was reasonable for fast dissolution – high solubility media, but it underpredicted the dissolution rate in a low solubility situation. This underprediction was probably due to the relative velocity being too low when only tangential velocity was included, without the impact of axial flow and gravitational effects. Consequently, the different hydrodynamic environment for sedimented vs suspended particles is not considered in the current simulations. This highlights the need to identify optimal hydrodynamic inputs for situations where dissolution is slower.

Funding

This work was supported by Science Foundation Ireland (SFI), co-funded under the European Regional Development Fund (Grant number 12/RC/2275_P2).

Credit author statement

Marina Navas-Bachiller: Methodology, Investigation, Verification, Writing, Visualisation.

Tim Persoons: Conceptualisation, Methodology, Software, Resources, Writing, Supervision, Funding Acquisition

Deirdre M D'Arcy: Conceptualisation, Methodology, Verification, Resources, Writing, Supervision, Project Administration, Funding Acquisition

Declaration of Competing interest

The authors declare no conflict of interests in this work.

Acknowledgements

SSPC, The Science Foundation Ireland Research Centre for Pharmaceuticals. We would like to acknowledge Prof Anne Marie Healy and Dr. Amelia Ultimo for assistance in the surface area analysis.

References

Alsenz, J., Kansy, M, 2007. High throughput solubility measurement in drug discovery and development. Advanced Drug Delivery Reviews 59, 546–567. https://doi.org/10.1016/j.addr.2007.05.007.

Bai, G., Wang, Y., Armenante, P.M., 2011. Velocity profiles and shear strain rate variability in the USP Dissolution Testing Apparatus 2 at different impeller agitation speeds. International Journal of Pharmaceutics 403, 1–14. https://doi.org/10.1016/j.ijpharm.2010.09.022.

Bai, G., Armenante, P.M., Plank, R.V., Gentzler, M., Ford, K., Harmon, P, 2007. Hydrodynamic Investigation of USP Dissolution Test Apparatus II. Journal of Pharmaceutical Science 96, 2327–2349. https://doi.org/10.1002/jps.20818.

Baxter, J.L., Kukura, J., Muzzio, F.J, 2005. Hydrodynamics-induced variability in the USP apparatus II dissolution test. International Journal of Pharmaceutics 292, 17–28. https://doi.org/10.1016/j.ijpharm.2004.08.003.

Bergman, T.L., Lavine, A.S, Incropera, F.P., Dewitt, D.P., 2011. Fundamentals Of Heat And Mass Transfer. John Wiley & Sons.

Butler, J. M., Dressman, J. B. The Developability Classification System : Application of Biopharmaceutics Concepts to Formulation Development. 99, 4940-4954 (2010). 10.1002/jps.22217.

Cammarn, S.R., Sakr, A., 2000. Predicting dissolution via hydrodynamics : salicylic acid tablets in flow through cell dissolution. International Journal of Pharmaceutics 201, 199–209. https://doi.org/10.1016/S0378-5173(00)00415-4.

Cristofoletti, R., Dressman, J.B., 2017. Dissolution Methods to Increasing Discriminatory Power of In Vitro Dissolution Testing for Ibuprofen Free Acid and Its Salts. Journal of Pharmaceutical Sciences. 106, 92–99. https://doi.org/10.1016/j.xphs.2016.06.001.

Cristofoletti, R., Dressman, J.B., 2016. Matching phosphate and maleate buffer systems for dissolution of weak acids: Equivalence in terms of buffer capacity of bulk solution or surface pH? European Journal of Pharmaceutics and Biopharmaceutics 103, 104–108. https://doi.org/10.1016/j.ejpb.2016.03.024.

D'Arcy, D.M., Liu, B., Bradley, G., Healy, A.M., Corrigan, O.I., 2010. Hydrodynamic and Species Transfer Simulations in the USP 4 Dissolution Apparatus : Considerations for Dissolution in a Low Velocity Pulsing Flow. Pharmaceutical Research 27, 246–258. https://doi.org/10.14227/DT180411P6.

D'Arcy, D.M., Liu, B., Persoons, T., Corrigan, O.I., 2011. Hydrodynamic complexity induced by the Pulsing Flow Field in USP Dissolution Apparatus 4. Dissolution Technologies 6–13. https://doi.org/10.14227/DT180411P6.

D'Arcy, D.M., Persoons, T, 2019. Understanding the Potential for Dissolution Simulation to Explore the Effects of Medium Viscosity on Particulate Dissolution. AAPS PharmSciTech. 1-13 https://doi.org/10.1208/s12249-018-1260-4.

D'Arcy, D.M., Persoons, T., 2011. Mechanistic Modelling and Mechanistic Monitoring : Simulation and Shadowgraph Imaging of Particulate Dissolution in the Flow-Through Apparatus. Journal of Pharmaceutical Science 100, 1102–1115. https://doi.org/10.1002/jps.22337.

FDA, 2017. Waiver of In Vivo Bioavailability and Bioequivalence Studies for Immediate-Release Solid Oral Dosage Forms Based on a biopharmaceutics classification system. Guidance for Industry, FDA Centre for Drug Evaluation and Research (CDER), US Department of Health and Human Services.

Healy, Anne Marie, Corrigan, Owen M, 1992. Predicting the dissolution rate of ibuprofen-acidic excipient compressed mixtures in reactive media. International Journal of Pharmaceutics 84, 167–173. https://doi.org/10.1016/0378-5173(92)90057-9.

Higuchi, M., Terada, K., Sugano, K, 2015. Coning phenomena under laminar flow. European Journal of Pharmaceutical Sciences 80, 53–55. https://doi.org/10.1016/j.ejps.2015.08.004.

Hintz, J.R., Johnson, K.C, 1989. The effect of particle size distribution on dissolution rate and oral absorption. International Journal of Pharmaceutics 51, 9–17. https://doi.org/10.1016/0378-5173(89)90069-0.

Johnson, K.C., 2012. Comparison of Methods for Predicting Dissolution and the Theoretical Implications of Particle-Size-Dependent Solubility. Journal of Pharmaceutical Sciences 101, 681–689. https://doi.org/10.1002/jps.22778.

Krieg, B.J., Taghavi, S.M., Amidon, G.L., Amidon, G.E., 2015. In Vivo Predictive Dissolution: Comparing the Effect of Bicarbonate and Phosphate Buffer on the Dissolution of Weak Acids and Weak Bases. Journal of Pharmaceutical Science 104, 2894–2904. https://doi.org/10.1002/jps.24460.

Kukura, J., Arratia, P.E., Szalai, E.S., Muzzio, F.J., 2003. Engineering Tools for Understanding the Hydrodynamics of Dissolution Tests. Drug Development and Industrial Pharmacy 29, 231–239. https://doi.org/10.1081/DDC-120016731.

Kukura, J., Baxter, J.L., Muzzio, F.J., 2004. Shear distribution and variability in the USP Apparatus 2 under turbulent conditions. International Journal of Pharmaceutics 279, 9–17. https://doi.org/10.1016/j.ijpharm.2004.03.033.

Levis, K.A., Lane, M.E., Corrigan, O.I, 2003. Effect of buffer media composition on the solubility and effective permeability coefficient of ibuprofen. International Journal of Pharmaceutics 253, 49–59. https://doi.org/10.1016/S0378-5173(02)00645-2.

Loisios-Konstantinidis, I., Cristofoletti, R., Fotaki, N., Turner, D.B., Dressman, J., 2020. Establishing virtual bioequivalence and clinically relevant specifications using in vitro biorelevant dissolution testing and physiologically-based population pharmacokinetic modeling. case example : Naproxen. European Journal of Pharmaceutical Sciences 143, 105170.

McCarthy, L.G., Bradley, G., Sexton, J.C., Corrigan, O.I., Healy, A.M., 2004. Computational Fluid Dynamics Modeling of the Paddle Dissolution Apparatus : Agitation Rate, Mixing Patterns, and Fluid Velocities. AAPS PharmSciTech 5. https://doi.org/10.1208/pt050231.

McCarthy, L.G., Kosiol, C., Healy, A.M., Bradley, G., Sexton, J.C., Corrigan, O.I., 2003. Simulating the Hydrodynamic Conditions in the United States Pharmacopeia Paddle Dissolution Apparatus. AAPS PharmSciTech 4, 1–16. https://doi.org/10.1208/pt040222.

Mills, Anthony F., Boehm, R.F., et al., 1999. Mass Transfer. In: Kreith, Frank (Ed.), Heat and Mass Transfer in: Mechanical Engineering Handbook. CRC Press.

Okazaki, A., Mano, T., Sugano, K, 2008. Theoretical Dissolution Model of Poly-Disperse Drug Particles in Biorelevant Media. Journal of Pharmaceutical Sciences 97, 1843–1852. https://doi.org/10.1002/jps.21070.

Pathak, S.M., Ru, A., Kostewicz, E.S., Patel, N., Turner, D.B., Jamei, M., 2017. Model-Based Analysis of Biopharmaceutic Experiments To Improve Mechanistic Oral Absorption Modeling: An Integrated in Vitro in Vivo Extrapolation Perspective Using Ketoconazole as a Model Drug. Molecular Pharmaceutics 14, 4305–4320. https://doi.org/10.1021/acs.molpharmaceut.7b00406.

Potthast, H., Dressman, J.B., Junginger, H.E., Midha, K.K., Oeser, H., Shah, V.P., Vogelpoel, H., Barends, D.M., 2005. Biowaiver Monographs for Immediate Release Solid Oral Dosage Forms : Ibuprofen. Journal of Pharmaceutical Sciences 94, 2121–2131. https://doi.org/10.1002/jps.20444.

Siepmann, J., Siepmann, F, 2013. Mathematical modeling of drug dissolution. International Journal of Pharmaceutics 453, 12–24. https://doi.org/10.1016/j.ijpharm.2013.04.044.

Sugano, K., 2009. Introduction to computational oral absorption simulation. Drug Metabolism & Toxicology 5, 259–293. https://doi.org/10.1517/17425250902835506.

Sugano, K., 2008. Theoretical comparison of hydrodynamic diffusion layer models used for dissolution simulation in drug discovery and development. International Journal of Pharmaceutics 363, 73–77. https://doi.org/10.1016/j.ijpharm.2008.07.002.

Todaro, V., Persoons, T., Groves, G., Healy, A.M, D'Arcy, D.M, 2017. Characterization and Simulation of Hydrodynamics in the Paddle, Basket and Flow-Through Dissolution Testing Apparatuses - A Review. Dissolution Technologies. 24, 24–36. dx.doi.org/10.14227/DT240317P24.

United States Pharmacopeia Convention (2021). United States Pharmacopeia and National Formulary (USPNF 2021 Issue 3 (4)).

Van der Vossen, A.C., Hanff, L.M., Vulto, A.G., Fotaki, N, 2019. Potential prediction of formulation performance in paediatric patients using biopharmaceutical tools and simulation of clinically relevant administration scenarios of nifedipine and lorazepam. British Journal of Clinical Pharmacology 85, 1728–1739. https://doi.org/10.1111/bcp.13956.

Wang, J., Flanagan, D.R, 1999. General Solution for Diffusion-Controlled Dissolution of Spherical Particles. 1. Theory. Journal of Pharmaceutical Science 88, 731–738. https://doi.org/10.1021/js980236p.

Wang, Y., Abrahamsson, B., Lindfors, L., Brasseur, J.G, 2012. Comparison and Analysis of Theoretical Models for Diffusion- Controlled Dissolution. Molecular Pharmaceutics 9, 1052–1066. https://doi.org/10.1021/mp2002818.